Suppression of Apoptosis by Nitric Oxide via Inhibition of Interleukin-1β–converting Enzyme (ICE)-like and Cysteine Protease Protein (CPP)-32–like Proteases

By Stefanie Dimmeler, Judith Haendeler, Michael Nehls, and Andreas M. Zeiher

From the Molecular Cardiology Group, Department of Internal Medicine IV, University of Frankfurt, Germany

Summary

Physiological levels of shear stress alter the genetic programm of cultured endothelial cells and are associated with reduced cellular turnover rates and formation of atherosclerotic lesions in vivo. To test the hypothesis that shear stress (15 dynes/cm^2) interferes with programmed cell death, apoptosis was induced in human umbilical venous cells (HUVEC) by tumor necrosis factor-α (TNF-α). Apoptosis was quantified by ELISA specific for histone-associated DNA-fragments and confirmed by demonstrating the specific pattern of internucleosomal DNA-fragmentation. TNF-α (300 U/ml) mediated increase of DNA-fragmentation was completely abrogated by shear stress (446 ± 121% versus 57 ± 11%, $P < 0.05$). This anti-apoptotic activity of shear stress decreased after pharmacological inhibition of endogenous nitric oxide (NO)-synthase by N^G-monomethyl-l-arginine and was completely reproduced by exogenous NO-donors.

The activation of interleukin-1β–converting enzyme (ICE)-like and cysteine protease protein (CPP)-32-like cysteine proteases was required to mediate TNF-α–induced apoptosis of HUVEC. Endothelial-derived nitric oxide (NO) as well as exogenous NO donors inhibited TNF-α–induced cysteine protease activation. Inhibition of CPP-32 enzyme activity was due to specific S-nitrosylation of Cys 163, a functionally essential amino acid conserved among ICE/CPP-32–like proteases. Thus, we propose that shear stress-mediated NO formation interferes with cell death signal transduction and may contribute to endothelial cell integrity by inhibition of apoptosis.

One of the most striking features of atherosclerosis is the focal nature of the disease. Atherosclerotic lesions preferentially develop in regions such as bends and bifurcations, where blood flow is disturbed with flow separation and, where shear stress is low and unsteady (1). The topographical association of regions with low shear stress with increased cell turnover rates at lesion-prone sites in the arterial tree (2) suggests an important link between local hemodynamics and the associated wall shear stress and the pathobiologic processes leading to endothelial cell injury and atherosclerosis.

Cellular injury may result in either necrosis or apoptosis. Apoptosis or programmed cell death is an essential mechanism for the maintenance of homeostasis in multicellular organisms (3). Apoptosis refers to the morphological alterations exhibited by "actively" dying cells that include cell shrinkage, membrane blebbing, chromatin condensation, and DNA fragmentation (3). Apoptotic cell death can result either from developmentally controlled activation of endogenous execution programs or from transduction of death signals triggered by a wide variety of exogenous stimuli (4). One major path in the cell suicide program requires the activation of cysteine proteases of the interleukin-1β–converting enzyme (ICE)[1]-like and cysteine protease protein (CPP)-32–like family, homologous to the product of the *Caenorhabditis elegans* cell death gene *ced 3* (5, 6).

We and others have previously shown, that the inflammatory cytokine tumor necrosis factor-α (TNF-α) affects endothelial cell viability and induces apoptosis in vitro in bovine and porcine endothelial cells (7). Because vascular wall shear stress alters the genetic growth program of cultured endothelial cells (8), reduces endothelial cell turnover rates (2, 9), and the development of atherosclerotic lesions in vivo (1, 10, 11), we hypothesized that shear stress may interfere with apoptosis of endothelial cells. In addition, since shear stress is closely correlated with endothelial cell nitric oxide (NO) production, we further investigated and

---

[1]*Abbreviations used in this paper:* AFC, 7-amino-4-trifluoro-methylcoumarin; AMC, 7-amino-4-coumarin; CCP, cysteine protease protein; DTNB, 5,5′dithiobis (2-nitrobenzoate); eNOS, endothelial NO-synthase; HUVEC, human umbilical venous endothelial cells; ICE, interleukin-1β-converting enzyme; LDH, lactate-dehydrogenase; LNMA, N^G-monomethyl-l-arginine; MTT, 3-(4,5-dimethylthiazol-2-yl)-2,5-diphenyltetrazolium bromide; NO, nitric oxide; SNP, sodium nitroprusside; SNAP, S-nitrosopenicillamine.

identified a potential autocrine mechanism of NO for mediating the anti-apoptotic effects of shear stress.

Materials and Methods

Human umbilical venous endothelial cells (HUVEC), endothelial basal medium, and supplements were purchased from Cell Systems/Clonetics (Solingen, Germany) and FCS from Gibco (Berlin, Germany). [^{32}P]dCTP was delivered by Amersham (Braunschweig, Germany). Klenow polymerase and cell death detection ELISA were from Boehringer Mannheim (Mannheim, Germany). ICE- and CPP32-substrates and inhibitors were delivered by Bachem (Heidelberg, Germany).

Cell Culture and Shear Stress Exposure. HUVEC were cultured in endothelial basal medium supplemented with hydrocortisone (1 µg/ml), bovine brain extract (3 µg/ml), gentamicin (50 µg/ml), amphotericin B (50 µg/ml), epidermal growth factor (10 µg/ml), and 10% fetal calf serum until the third passage. After detachment with trypsin, cells were grown for at least 18 h. Confluent monolayers of HUVEC were grown onto 6-cm wells and exposed to laminar fluid flow in a cone-and-plate apparatus as previously described (12). A constant shear stress of 15 dynes/cm^2 was used in all experiments to simulate physiological shear stress (8, 12).

DNA Fragmentation. Cells were scraped off the plates and centrifuged at 700 *g* for 10 min, washed with PBS and resuspended in incubation buffer. The histone-associated DNA-fragments were linked to the anti-histone antibody from mouse and the DNA-part of the nucleosome to the anti-DNA-peroxidase. The amount of peroxidase retained in the immunocomplex was determined photometrically with 2,2′-azino-di-(3-ethylbenzthiazoline sulfonate) as a substrate.

For the internucleosomal DNA-laddering, 1×10^6 cells were removed from culture flask, washed with PBS and incubated in lysis buffer (5 mM Tris/HCl, pH 8, 20 mM EDTA and 0.5% Triton X-100) for 15 min at 4°C. Then samples were incubated with RNase A for 1 h at 37°C, followed by addition of a final concentration of 0.5 mg/ml proteinase K and 1% SDS. The samples were then incubated overnight at 65°C. After isolation of DNA by phenol-chloroform extraction the DNA was precipitated with 70% isopropanol and 0.1 M NaCl. The resulting pellet was resolved in TE buffer (10 mM Tris/HCl, pH 8, 1 mM EDTA) and the DNA samples were incubated with 5 U of Klenow polymerase, 0.5 µCi [^{32}P]dCTP in the presence of 10 mM Tris/HCl, pH 7.5, and 5 mM MgCl$_2$ for 10 min at room temperature according to Rösl et al. (13). The reaction was terminated by addition of 10 mM EDTA and the unincorporated nucleotides were removed with Sephadex G-50 spin columns. Labeled DNA fragments were separated on a 1.0% agarose gel, transferred to nitrocellulose membranes, and exposed to x-ray film.
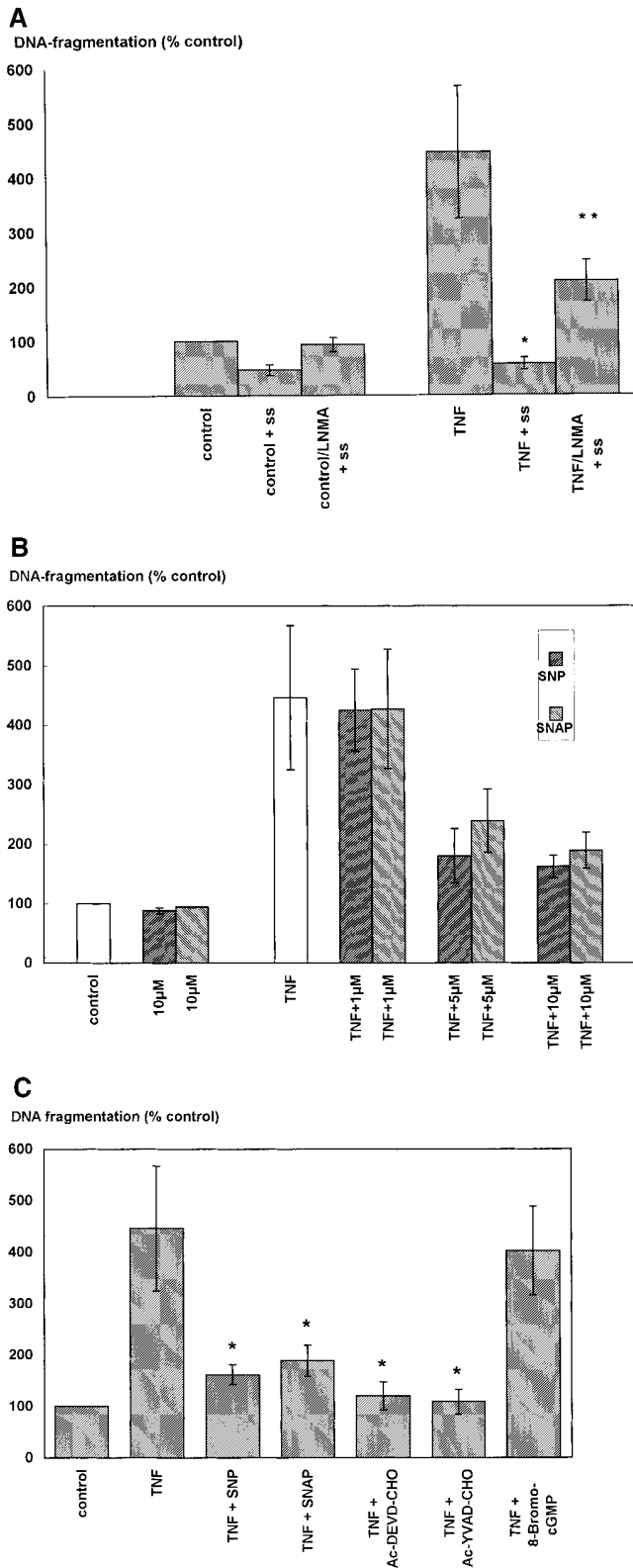
Determination of Cell Viability and LDH Release. Cell viability was assessed as described previously (14). HUVEC (1×10^5 cells/ml) were incubated in microtiter plates for 18 h with apoptotic stimuli. Then, cells were treated with 3-(4,5-dimethylthiazol-2-yl)-2,5-diphenyltetrazolium bromide (MTT, 0.5 mg/ml) for 4 h at 37°C, medium was removed and cells were lysed with 2-isopropanol containing 0.04 M HCl. The metabolized MTT was determined photometrically (595 nm).

For measurement of lactate-dehydrogenase (LDH) levels, a kit was used (Boehringer Mannheim, Germany). 1×10^5 cells were seeded into 12-well plates. The cell culture supernatant was incubated with pyruvate and NADH and the LDH activity was determined photometrically according to the manufacturers protocols.

ICE and CPP32 Enzyme Activity. For detection of ICE and CPP32-activity, HUVEC (1×10^6 cells) were lysed in buffer (1% Triton X-100, 0.32 M sucrose, 5 mM EDTA, 1 mM PMSF, 1 µg/ml aprotinin, 1 µg/ml leupeptin, 2 mM DTT, 10 mM Tris/HCl, pH 8) for 15 min, 4°C, followed by centrifugation (20,000 *g*, 2 min). CPP-32–like activity was detected in resulting supernatants by measuring the proteolytic cleavage of the fluorogenic substrate 7-amino-4-coumarin (AMC)-DEVD (15) and AMC as standard in assay buffer (100 mM Hepes, 10% sucrose, 0.1% CHAPS, pH 7.5, 1 mM PMSF, 1 µg/ml aprotinin, 1 µg/ml leupeptin, 2 mM DTT) using an excitation wavelength of 380 nm and an emmission wavelength of 460 nm. Similarly, ICE–like activity was measured with 14 µM 7-amino-4-trifluoro-methylcoumarin (AFC)-conjugated YVAD-peptide as substrate and AFC as standard at an excitation wavelength of 400 nm versus an emmission wavelength of 505 nm (16). Specificity for CPP-32/ICE–like enzymatic activity was demonstrated by inhibition with 10 nM Ac-DEVD-CHO and 10 µM Ac-YVAD-CHO, respectively (15–17). Protein content was analyzed using the Biorad assay (Biorad, München, Germany). The specific activity of CPP32- and ICE-like protease activity in homogenates of control cells was 3.6 ± 0.6 pmol AMC × mg protein^{-1} × min^{-1} and 2.7 ± 1.4 pmol AFC × mg protein^{-1} × min^{-1}, respectively.

Cloning and Purification of ICE- and CPP-32 Subunits. The human CPP32 p17 and p12 subunits and the human ICE p10 and p20 subunits were amplified by PCR with oligonucleotides that were synthesized to contain BamH1 and SacI restriction sites and were cloned into the respective sites of pQE30 (Qiagen, Hilden, Germany) containing a 6× histidine affinity tag. The cys 163-mutated p17 was generated by amplification of pQE30-p17 by PCR with the following primers: primer 1, 5′-GGAGGATC-CCCTGGACAACAG-3′and primer 2, 5′-CTCAATGCCACAG-TCCAGTTCTGTACCACGG**CC**GGCCTGAAT (exchanged base pairs in bold) followed by an additional PCR with primer 1 and primer 3:5′-GTCGAGCTCAATGCCACAGTC containing the SacI restriction site. Clones with verified sequence were expressed in *Escherichia coli. E. coli* were lysed in buffer (8 M urea, 0.1 M Na-phosphate, 0.01 M Tris/HCl, pH 8) and the subunits were purified by metal chelate affinity chromatography with Ni^{2+}-nitrilo-triacetic acid (Ni-NTA) resins. After elution with 200 mM EDTA, the isolated subunits were renatured by dialysis overnight (18) and protein concentration was determined with the Biorad assay with bovine serum albumine as standard. We obtained ~6 mg purified protein/120 mg crude extract. Enzymatic activity of the reconstituted CPP-32 (p17 and p12) and ICE subunits (p10 and p20) was monitored as outlined above. The specific activity of reconstituted ICE and CPP-32 in dialyzed crude homogenates was 720 ± 102 pmol AMC × mg protein^{-1} × min^{-1} and 318 ± 78 pmol AFC × mg protein^{-1} × min^{-1}, respectively, whereas the purified reconstituted proteins exhibited a specific activity of 7,805 ± 200 pmol AMC × mg protein^{-1} × min^{-1} and 2,838 ± 219 pmol AFC × mg protein^{-1} × min^{-1}, respectively.

S-Nitrosylation. For demonstration of S-nitrosylation, bacterially expressed CPP-32 wild-type p17 subunit (p17 wt) and Cys 163-mutated p17 subunit (p17 mt) were purified as described above and p17 subunits were renatured by dialysis in 10 mM Tris/HCl, pH 7.5, overnight (18). Then, 0.5 mg protein was incubated in 30 mM Tris/HCl, pH 7.5, with NO released nonenzymatically by NaNO$_2$ or sodium nitroprusside (SNP) (19, 20) for the time indicated and again was dialysed overnight. S-nitrosylation was determined spectrophotometrically at 335 nm using an extinction coefficient of 3,869 mol^{-1} × cm^{-1} (19, 20), titration of SH-groups was carried out with excess of 5,5′dithiobis(2-nitroben-

A

DNA-fragmentation (% control)

B

DNA-fragmentation (% control)

C

DNA fragmentation (% control)

Figure 1. Inhibition of TNF-α–induced apoptosis by shear stress, nitric oxide and ICE-like and CPP-32–like protease inhibitors in human endothelial cells. (*A*) HUVEC were incubated with LNMA (1 mM) and/or TNF-α (300 U/ml) for 18 h with or without additional shear stress (*ss*) and DNA fragmentation was determined. Results are means ± SE, with *$P <0.05$ versus TNF-α; **$P <0.05$ versus TNF-α + shear stress. (*B*) Dose-

zoate) (DTNB) at 412 nm with an extinction coefficient of 13,600 $mol^{-1} \times cm^{-1}$ (19).

Western Blot Analysis. For Western blotting proteins were prepared and quantified as described above and protein samples (60 μg) were resolved on 8% sodium dodecyl sulfate polyacrylamide-gels and blotted on membranes. Membranes were blocked with 2% bovine serum albumin overnight and were incubated with anti-endothelial NO-synthase antibody (1:2,500; Dianova, Hamburg, Germany) for 1 h and anti-mouse horseradish peroxidase conjugate as the second antibody. Next, the membranes were stained with enhanced chemiluminescence. The autoradiographies were scanned and semiquantitatively quantified.

Results and Discussion

Shear Stress Prevents TNF-α-induced Apoptosis in Human Endothelial Cells. TNF-α triggered apoptosis in HUVEC in a time-dependent fashion with maximum effects after 18 h exposure (Fig. 1 *A*). There was no increase in lactate dehydrogenase activity by TNF-α treatment excluding the induction of cell necrosis (data not shown). Exposure of HUVEC to physiological levels (15 dynes/cm^2) of laminar shear stress dramatically reduced basal and TNF-α–triggered apoptosis. Shear stress results in an immediate increase in endothelial NO production and further chronically enhances NO synthesis by increasing endothelial NO-synthase expression (12, 21). In our experimental setting, NO synthesis measured by cGMP levels increased more than twofold 5 min after the onset of shear stress. Furthermore, increased protein levels of endothelial NO-synthase (eNOS) were sustained for 18 h of shear stress exposure up to 150 ± 10% compared with controls. Although TNF-α slightly reduced eNOS protein levels at baseline, shear stress increased eNOS protein to a similar extent in the presence of TNF-α (132 ± 4%). Inhibition of NO formation by N^G-monomethyl-l-arginine (LNMA) significantly inhibited the effect of shear stress on the reduction of TNF-α–mediated cell death and completely restored basal apoptosis (Fig. 1 *A*). Thus, physiological concentrations of endogenous NO appear to be capable of suppressing TNF-α–triggered apoptosis of HUVEC. To demonstrate the antiapoptotic potential of NO, we investigated the effect of exogenous NO donors. Coincubation with SNP or S-nitrosopenicillamine (SNAP) dose-dependently decreased TNF-α–triggered apoptosis (Fig. 1 *B*). NO donors did not affect apoptosis in the absence of TNF-α (Fig. 1 *B*). Low concentrations up to 50 μM of NO-donors were shown to be protective, whereas higher concentrations (>300 μM) revealed the known proapoptotic effect (22) (data not shown). TNF-α–induced apoptosis corre-

dependent inhibition of TNF-α–induced apoptosis by the NO donors SNP and SNAP. HUVEC were incubated with SNP and SNAP with or without TNF-α (300 U/ml) for 18 h and DNA fragmentation was measured. (*C*) Effect of protease inhibitors or NO donors on TNF-α induced apoptosis after 18 h of incubation. Substances were added just before TNF-α addition in the following concentrations: SNP and SNAP (10 μM); ICE-like protease inhibitor Ac-YVAD-CHO and CPP-32–like inhibitor Ac-DEVD-CHO (100 μM); 8-bromo-cGMP (1 mM). Results are means ± SE, with *$P <0.05$ versus TNF-α.

A

CPP-32-like activity (% control)

B
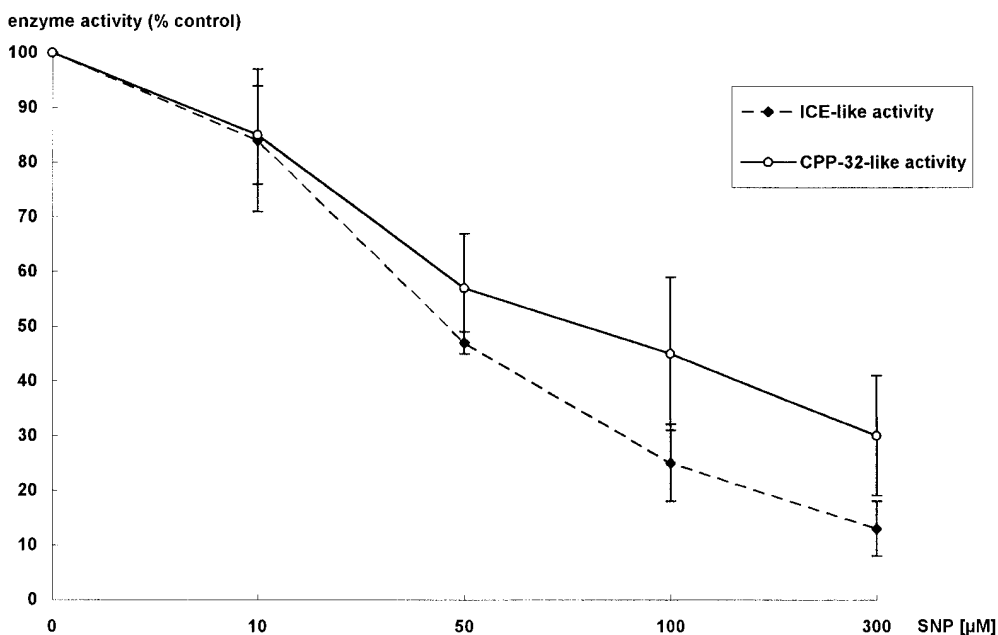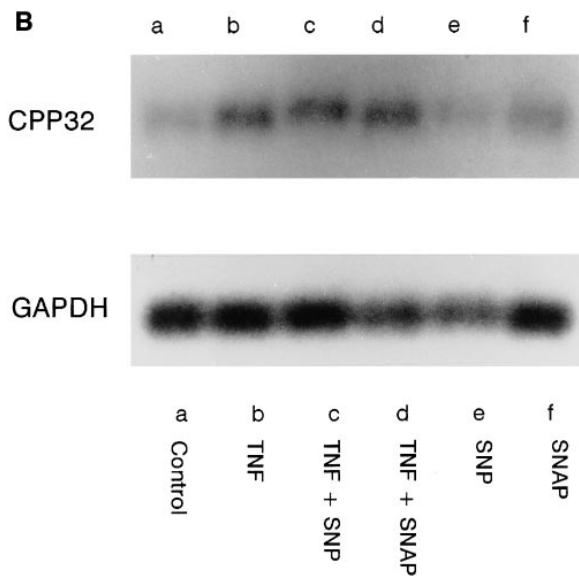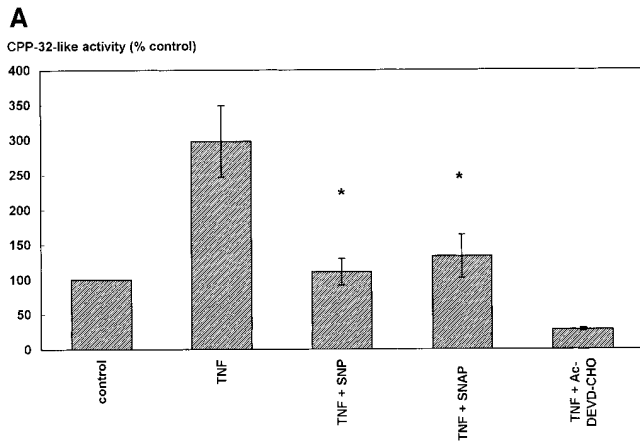

lated with a decrease of cell viability by $22 \pm 6\%$, which was completely prevented by NO donors. The inhibition of TNF-α–induced apoptosis by NO appeared to be independent of elevated cGMP levels, since the cGMP analogue 8-bromo-cGMP did not affect DNA fragmentation (Fig. 1 C).

TNF-α-induced Apoptosis Depends on ICE/CPP32-like Proteases Activity. To identify the antiapoptotic mechanism of NO, we investigated the involvement of ICE/CPP32–like proteases in TNF-α–mediated apoptosis in HUVEC. Addition of the tetrapeptide inhibitors Ac-YVAD-CHO and Ac-DEVD-CHO, which are specific inhibitors of ICE-like (6, 17) and CPP-32–like (17, 23) proteases, respectively, abrogated TNF-α–triggered apoptosis in HUVEC in a dose-dependent manner with maximum effects at 100 μM (Fig. 1 C). The inhibition of TNF-α–triggered apoptosis by NO donors was equipotent to the effects of the specific tetrapeptide protease inhibitors as assessed by densitometric measurement of DNA fragmentation (Fig. 1 C).

Next, we measured ICE/CPP-32–like proteases activity in HUVEC incubated for 18 h in the presence of TNF-α (300 U/ml) and SNP or SNAP (10 μM). ICE- and CPP-32–like protease activities were directly determined in the homogenate. Exogenous NO completely suppressed the increase in CPP-32–like protease activity induced by TNF-α (Fig. 2 A). Similarly, endogenous NO, induced by shear stress, also inhibited TNF-α stimulation of both proteases ($P = 0.04$), an effect completely reversed by addition of the

Figure 2. (A) CPP-32–like activity in HUVEC treated with NO donors (10 μM) or Ac-DEVD (100 μM) and TNF-α (300 U/ml) for 18 h. (B) Northern blot analysis of CPP32. RNA from HUVEC was prepared after 6 h of incubation with TNF-α (300 U/ml), SNP and SNAP (10 μM) as indicated. 10 μg of total RNA was resolved, blotted and sequentially hybridized to full-length human cDNA of CPP-32 and GAPDH.

enzyme activity (% control)

Figure 3. Direct inhibition of ICE-like and CPP-32–like enzyme activity by NO. Inhibition of ICE-like and CPP-32–like activity in cell homogenates by preincubation with various concentrations of SNP for 5 min. Cell homogenates were obtained from TNF-α–stimulated HUVEC (300 U/ml for 18 h).
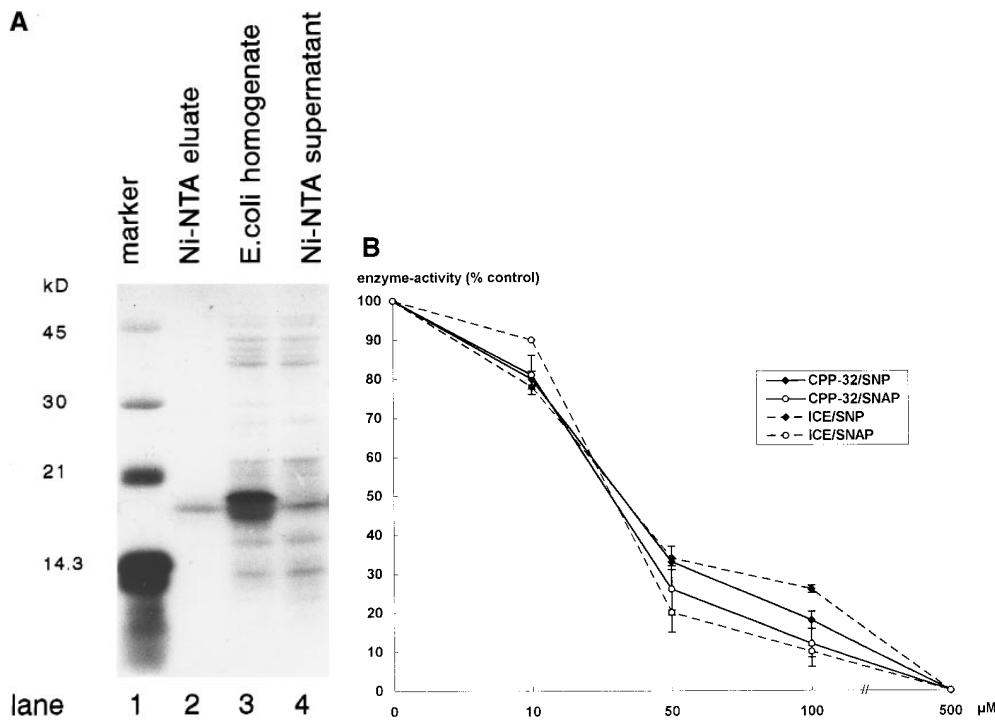
Figure 4. Purification of p17 subunits and direct inhibition of reconstituted CPP-32- and ICE-subunits by NO. (*A*) Silver stain of the crude homogenates before purification (60 μg; lane *3*), the unbound fraction of the Ni-NTA columns (60 μg; lane *4*) and the purified CPP-32 p17 subunit (10 μg; lane *2*) separated by a 12% SDS–polyacrylamide gel. (*B*) Inhibition of cloned, purified and reconstituted CPP-32 and ICE by incubation with SNP or SNAP for 1 h.

NO-synthase inhibitor LNMA (99 ± 3% of TNF-induced CPP-32–like activity).

NO Inhibits ICE/CPP-32–like Protease Activity. Having demonstrated that both endogenous as well as exogenous NO inhibits the TNF-α–induced activation of ICE/CPP-32–like proteases in intact cells, we next sought to examine potential mechanisms, by which NO interferes with CPP-32 activity. TNF-α increased the steady state expression of CPP-32 mRNA in HUVEC after 6 h of incubation. However, neither the basal level of CPP-32 mRNA nor the TNF-α–induced increase was affected in the presence of NO donors (Fig. 2 *B*) suggesting a posttranscriptional mechanism responsible for NO-mediated inhibition of CPP-32 activation. Therefore, we investigated the CPP-32 protein as a potential direct target for NO-mediated interference. In the next set of experiments, we treated homogenates of TNF-α–stimulated endothelial cells with SNP and SNAP. Both NO donors led to a dose-dependent decrease in TNF-α induced CPP-32–like protease activity with an IC50 value of about 50 μM for SNP (Fig. 3 *A*), when added 3 min before starting the enzymatic reaction. This effect was due to the NO-releasing capacity of the compounds used, since controls with sodium cyanide (300 μM) did not affect CPP-32–like enzyme activity (83 ± 17% of control). Similarly, ICE-like proteases activity was inhibited with equal efficiency (Fig. 3 *A*).

Direct S-Nitrosylation of ICE/CPP32–like Proteases Downregulates Enzyme Activity. ICE- and CPP-32–like proteases possess a highly conserved and functionally essential cysteine within their active center (5, 6, 23). Since S-nitrosylation is a well-established mechanism, by which NO can inhibit enzyme activity (19, 24, 25), we biochemically analyzed a potentially direct interaction of NO with CPP-32.

Upon activation, proteolytical cleavage of CPP-32 releases two subunits, p12 and p17, which heterodimerize to form the active protease (23). The p17 subunit contains the reactive cysteine group at position 163 in its active center (23). Therefore, both subunits were separately cloned, bacterially expressed, and purified to homogeneity as demonstrated by silver staining (Fig. 4 *A*). S-nitrosylation of the p17 subunit was performed and detected according to Stamler (20). Table 1 illustrates that NO released by $NaNO_2$ or SNP time-dependently S-nitrosylated one thiol group per molecule p17. The S-nitrosylation correlated with the reduction of one thiol-group per molecule p17 detectable by DTNB (Table 1). These findings were further substantiated by demonstrating that the isolated p17 subunit, but not the p12 subunit NO-dependently incorporated [^{32}P]NAD, a reaction being mediated by S-nitrosylation (19, 26) (data not shown). Similar results were obtained for the corresponding p10/p20 subunits of ICE (data not shown).

In vitro reconstitution of both the p17 with the separately expressed and purified p12 subunit of CPP32 as well as the p20 and p10 subunit of ICE exhibited potent CPP32 and ICE enzyme activity, respectively. S-nitrosylation of the p17-CPP32 or the p20-ICE subunit performed before reconstitution led to a complete inhibition of enzyme activity after SNP (500 μM)-induced S-nitrosylation for 60 min. Enzyme activity of both reconstituted heterodimers was dose-dependently reduced by NO donors with equal efficiencies (Fig. 4 *B*). Thus, S-nitrosylation of the p17 subunit of CPP-32 or the p20 subunit of ICE is associated with profound inhibition of enzyme activity.

The p17 subunit of CPP32 contains five cysteine groups. To identify the NO acceptor amino acid, we mutated the highly reactive Cys 163 to Ala 163 by PCR-cloning. No

Table 1. *S-nitrosylation of Bacterially Expressed CPP-32 Wild-type p17 Subunit (p17 wt) and Cys 163-mutated p17 (p17 mt)*

	p17 wt		p17 mt
	S-nitrosylation	Titration of SH-groups	Titration of SH-groups
	S-NO/protein	SH-groups/ protein	SH-groups/ protein
	mol/mol		
Control	0 ± 0	1.05 ± 0.06	0.08 ± 0.04
NaNO$_2$ (30 min)	0.55 ± 0.03	0.53 ± 0.04	ND
NaNO$_2$ (60 min)	1 ± 0.04	0.06 ± 0.03	ND
SNP (60 min)	0.99 ± 0.01	0.1 ± 0.09	ND

Data from three independent experiments are shown and expressed as means ± SE.

reactive SH group was detectable, when titrating the SH groups of the bacterially expressed p17 mutant (Table 1), suggesting that Cys 163 is the main cysteine group which is S-nitrosylated by NO. Interestingly, another mutant, Ser 120 to Gly 120, which abolished enzyme activity, but still contains all five cysteine residues, was not S-nitrosylated (data not shown), indicating that the ability to react with NO depends on the formation of an active center.

NO, produced at low levels, has been previously shown to inhibit apoptosis of human B cells, albeit the mechanisms involved have not been elucidated (27, 28). In contrast, other studies have found that high levels of NO induce apoptosis of macrophages (22). These effects of NO activity as a double-edged sword can be well rationalized. High concentrations of NO lead to direct DNA damage or exhibit cytotoxic effects (29), whereas low levels of NO inhibit apoptosis via posttranslational modification of ICE/CPP-32–like proteases by S-nitrosylation. The constitutively expressed endothelial cell nitric oxide synthase produces low levels of NO (12, 21, 29) suggesting that endothelial cell NO production may render endothelial cells resistant to a major trigger of apoptosis. Although low concentrations of exogenous NO were sufficient to prevent TNF-α–triggered apoptosis, the pharmacological inhibition of shear stress induced NO production did only partially reverse the TNF-α effect (see Fig. 1 *A*). This result suggests that shear stress utilizes additional NO-independent antiapoptotic mechanisms, which remain to be identified. Shear stress has previously been shown to modulate phosphorylation of tyrosine kinases (8) indicating activation of second messengers, which might interfere with cell death signal transduction. In addition, shear stress alters F-actin organization through regulation of focal adhesion-associated proteins in endothelial cells (8), which might play an additional role in mediating apoptosis (3, 4).

The function of NO to act as an intracellular control mechanism to protect endothelial cells from being driven into apoptosis under stimulation with TNF-α may have important pathophysiological implications. The endothelium plays a pivotal role as a gate keeper regulating recruitment of blood-borne cells during inflammation, atherosclerosis, and immune surveillance. Since TNF-α is a major inflammatory and/or immune cytokine, protection of TNF-α–induced apoptosis of endothelial cells by NO might importantly contribute to the integrity of the endothelial cell layer.

Moreover, since ICE-like and CPP-32–like proteases play a crucial role not only in TNF-α and APO-1/FAS–triggered apoptosis, but turn out to be of general importance in the apoptotic-signaling cascade (5, 17, 23), the potential of low level NO to modulate ICE/CPP-32-like proteases activity might have a general impact on the response of cells to death signals.

Address correspondence to Andreas M. Zeiher, Department of Internal Medicine IV, Division of Cardiology, University of Frankfurt, Theodor Stern-Kai 7, 60590 Frankfurt, Germany.

References

1. Ku, D.N., D.P. Giddens, C.K. Zarins, and S. Glagov. 1985. Pulsatile flow and atherosclerosis in the human carotid bifurcation. Positive correlation between plaque location and low oscillating shear stress. *Arteriosclerosis.* 5:293–302.
2. Caplan, B.A., and C.J. Schwartz. 1973. Increased endothelial cell turnover in areas of in vivo Evans Blue uptake in the pig aorta. *Atherosclerosi.s* 17:401–417.
3. Cohen, J.J. 1993. Apoptosis. *Immunol. Today.* 14:126–130.
4. Steller, H. 1995. Mechanisms and genes of cellular suicide. *Science (Wash. DC).* 267:1445–1449.
5. Kumar, S. 1995. ICE-like proteases in apoptosis. *Trends Biochem. Sci.* 20:198–202.
6. Thornberry, N.A., H.G. Bull, J.R. Calaycay, K.T. Chapman, A.D. Howard, M.J. Kostura, D.K. Miller, S.M. Molineaux, J.R. Weidner, J. Aunins et al. 1992. A novel heterodimeric cysteine protease is required for interleukin-1 beta processing in monocytes. *Nature (Lond.).* 356:768–774.
7. Robaye, B., R. Mosselmans, W. Fiers, J.E. Dumont, and P. Galand. 1991. Tumor necrosis factor induces apoptosis (programmed cell death) in normal endothelial cells in vitro. *Am. J. Pathol.* 138:447–453.
8. Malek, A.M., and S. Izumo. 1994. Molecular aspects of signal transduction of shear stress in the endothelial cell. *J. Hypertens.* 12:989–999.

9. Azumi, T., and J. O'Shea. 1994. Mechanism of deletion of endothelial cells during regression of the corpus luteum. *Lab. Invest.* 51:206–217.

10. Kohler, T.R., T.R. Kirkman, L.W. Kraiss, B.K. Zierler, and A.W. Clowes. 1991. Increased blood flow inhibits neointimal hyperplasia in endothelialized vascular grafts. *Circ. Res.* 69:1557–1565.

11. Nerem, R.M., D.G. Harrison, W.R. Taylor, and R.W. Alexander. 1993. Hemodynamics and vascular endothelial biology. *J. Cardiovasc. Pharmacol.* 21:S6–10.

12. Noris, M., M. Morigi, R. Donadelli, S. Aiello, M. Foppolo, M. Todeschini, S. Orisio, G. Remuzzi, and A. Remuzzi. 1995. Nitric oxide synthesis by cultured endothelial cells is modulated by flow conditions. *Circ. Res.* 76:536–543.

13. Rösl, F. 1992. A simple and rapid method for detection of apoptosis in human cells. *Nucleic Acids Res.* 20:5243.

14. Dimmeler, S., S. Brinkmann, and E. Neugebauer. 1995. Endotoxin-induced changes of endothelial cell viability and permeability: protective effect of a 21-aminosteroid. *Eur. J. Pharmacol.* 287:257–261.

15. Bump, N.J., M. Hackett, M. Hugunin, S. Seshagiri, K. Brady, P. Chen, C. Ferenz, S. Franklin, T. Ghayur, P. Li et al. 1995. Inhibition of ICE family proteases by baculovirus antiapoptotic protein p35. *Science (Wash. DC).* 269:1885–1888.

16. Thornberry, N.A. 1994. Interleukin-1 beta converting enzyme. *Methods Enzymol.* 244:615–631.

17. Enari, M., R.V. Talanian, W.W. Wong, and S. Nagata. 1996. Sequential activation of ICE-like and CPP32-like proteases during Fas-mediated apoptosis. *Nature (Lond.).* 380:723–726.

18. Ramage, P., D. Cheneval, M. Chvei, P. Graff, R. Hemmig, R. Heng, H.P. Kocher, A. Mackenzie, K. Memmert, L. Revesz et al. 1995. Expression, refolding, and autocatalytic proteolytic processing of the interleukin-1 beta-converting enzyme precursor. *J. Biol. Chem.* 270:9378–9383.

19. Molina y Vedia, L., B. McDonald, B. Reep, B. Brune, M. Di Silvio, T.R. Billiar, and E.G. Lapetina. 1992. Nitric oxide-induced S-nitrosylation of glyceraldehyde-3-phosphate dehydrogenase inhibits enzymatic activity and increases endogenous ADP-ribosylation. *J. Biol. Chem.* 267:24929–24932.

20. Stamler, J.S., D.I. Simon, O. Jaraki, J.A. Osborne, S. Francis, M. Mullins, D. Singel, and J. Loscalzo. 1992. S-nitrosylation of tissue-type plasminogen activator confers vasodilatory and antiplatelet properties on the enzyme. *Proc. Natl. Acad. Sci. USA.* 89:8087–8091.

21. Uematsu, M., Y. Ohara, J.P. Navas, K. Nishida, T. J. Murphy, R.W. Alexander, R.M. Nerem, and D.G. Harrison. 1995. Regulation of endothelial cell nitric oxide synthase mRNA expression by shear stress. *Am. J. Physiol.* 269:C1371–1375.

22. Messmer, U.K., M. Ankarcrona, P. Nicotera, and B. Brune. 1994. p53 expression in nitric oxide-induced apoptosis. *FEBS Lett.* 355:23–26.

23. Nicholson, D.W., A. Ali, N.A. Thornberry, J.P. Vaillancourt, C.K. Ding, M. Gallant, Y. Gareau, P.R. Griffin, M. Labelle, Y.A. Lazebnik et al. 1995. Identification and inhibition of the ICE/CED-3 protease necessary for mammalian apoptosis. *Nature (Lond.).* 376:37–43.

24. Stamler, J.S., D.I. Simon, J.A. Osborne, M.E. Mullins, O. Jaraki, T. Michel, D.J. Singel, and J. Loscalzo. 1992. S-nitrosylation of proteins with nitric oxide: synthesis and characterization of biologically active compounds. *Proc. Natl. Acad. Sci. USA.* 89:444–448.

25. Stamler, J.S. 1995. S-nitrosothiols and the bioregulatory actions of nitrogen oxides through reactions with thiol groups. *Curr. Top. Microbiol. Immunol.* 196:19–36.

26. Dimmeler, S., F. Lottspeich, and B. Brune. 1992. Nitric oxide causes ADP-ribosylation and inhibition of glyceraldehyde-3-phosphate dehydrogenase. *J. Biol. Chem.* 267:16771–16774.

27. Mannick, J.B., K. Asano, K. Izumi, E. Kieff, and J.S. Stamler. 1994. Nitric oxide produced by human B lymphocytes inhibits apoptosis and Epstein-Barr virus reactivation. *Cell.* 79:1137–1146.

28. Genaro, A.M., S. Hortelano, A. Alvarez, C. Martinez, and L. Bosca. 1995. Splenic B lymphocyte programmed cell death is prevented by nitric oxide release through mechanisms involving sustained Bcl-2 levels. *J. Clin. Invest.* 95:1884–1890.

29. Nathan, C. 1992. Nitric oxide as a secretory product of mammalian cells. *FASEB J.* 6:3051–3064.